The Astrophysical Journal, 622:959–964, 2005 April 1

ORIGINS OF THE $\frac{1}{4}$ keV SOFT X-RAY BACKGROUND

Eric C. Bellm[1] and John E. Vaillancourt[2]
Physics Department, University of Wisconsin, 1150 University Avenue, Madison, WI 53706
Received 2004 October 19; accepted 2004 December 21

ABSTRACT

Snowden and coworkers have presented a model for the $\frac{1}{4}$ keV soft X-ray diffuse background in which the observed flux is dominated by a $\sim 10^6$ K thermal plasma located in a 100–300 pc diameter bubble surrounding the Sun but has significant contributions from a very patchy Galactic halo. Halo emission provides about 11% of the total observed flux and is responsible for half of the H I anticorrelation. The remainder of the anticorrelation is presumably produced by displacement of disk H I by the varying extent of the Local Hot Bubble (LHB). The *ROSAT* R1 and R2 bands used for this work had the unique spatial resolution and statistical precision required for separating the halo and local components but provide little spectral information. Some consistency checks had been made with older observations at lower X-ray energies, but we have made a careful investigation of the extent to which the model is supported by existing sounding rocket data in the Be (73–111 eV) and B (115–188 eV) bands, where the sensitivities to the model are qualitatively different from the *ROSAT* bands. We conclude that the two-component model is well supported by the low-energy data. We find that these combined observations of the local component may be consistent with single-temperature thermal emission models in collisional ionization equilibrium if depleted abundances are assumed. However, different model implementations give significantly different results, offering little support for the conclusion that the astrophysical situation is so simple.

Subject headings: X-rays: diffuse background — X-rays: ISM

1. INTRODUCTION

Early observations of the $\frac{1}{4}$ keV diffuse X-ray background showed a strong anticorrelation with Galactic H I column density that suggested an extragalactic source absorbed by foreground interstellar gas. However, it gradually became apparent that (1) there is a large flux in the Galactic plane, although unit optical depth at $\frac{1}{4}$ keV is only 1×10^{20} H atoms cm^{-2}, (2) the apparent absorption cross sections observed at intermediate and high Galactic latitudes are much smaller than the calculated photoelectric values, and (3) the still softer B and Be bands show, on the average, almost identical variations with $N_{\rm H}$ despite absorption cross sections that should be 2–10 times larger (Table 1). These three observations were readily explained by a model in which the $\frac{1}{4}$ keV flux originates in an irregular Local Hot Bubble (LHB) of 100–300 pc extent surrounding the Sun (Sanders et al. 1977; McCammon & Sanders 1990). In this model, the X-ray–H I anticorrelation is produced by the displacement of neutral material by a 10^6 K plasma. Snowden et al. (1990) showed that H I column densities were consistent with the excavation of a standard plane-parallel disk by a uniform X-ray–emitting bubble of extent varying as required by the observed X-ray brightness. With the limited statistics available, the small variations in the X-ray band ratios appeared random and uncorrelated with $N_{\rm H\,I}$, as would be expected for this model with all emission in the foreground.

Some of the first diffuse background observations using the improved angular resolution of *ROSAT*, however, revealed shadowing of half the observed $\frac{1}{4}$ keV X-ray flux toward molecular clouds known to lie several hundred parsecs above the Galactic plane, showing that a significant part of the $\frac{1}{4}$ keV emission is from above the Galactic disk (e.g., Burrows & Mendenhall 1991; Snowden et al. 1991, 1994a). To account for this, Snowden et al. (1998, hereafter S98) proposed a multicomponent model that includes both a LHB and patchy halo emission absorbed by the intervening disk gas (see also Kuntz & Snowden 2000). They have estimated the halo contribution by fitting spatial variations in the R1 and R2 bands of the *ROSAT* all-sky survey to variations in the H I column density on angular scales too small for displacement to have an appreciable effect. The remainder is assumed to come from the LHB as before with no absorption. We refer to the latter part as the local R12 rate (R12 band = R1 + R2; see Fig. 1). A fixed contribution from extragalactic point sources was also included, described by a power law in energy.

S98 capitalized on the improved angular resolution ($\sim 12'$) and very good statistical precision of the *ROSAT* all-sky survey to isolate the effects of absorption and displacement and allow division of the observed flux into two components. However, the R1 and R2 bands have effective energies that differ by only a small fraction of their widths and provide limited spectral information (Fig. 1; Table 1). A 10^6 K plasma radiates strongly at lower energies as well, where the interstellar absorption cross sections are much larger. As yet there have been no useful satellite surveys at lower energies, and we must therefore rely on existing data from older sounding rocket surveys, despite their much poorer angular resolution and statistical precision. A series of 10 rocket flights from 1972 to 1982 completed an all-sky survey in the B band (115–188 eV), as well as a C-band equivalent to the *ROSAT* R12 band (McCammon et al. 1983). Additional sounding rocket flights between 1984 and 1988 made a total of 25 pointed observations at soft X-ray energies in the Be band (77–111 eV; Bloch et al. 1986; Edwards 1990; Juda et al. 1991). With their limited statistical precision, both sets of observations were consistent with the total flux in these bands originating in the LHB. However, the division of R12 intensity into local and halo components makes very specific predictions

[1] Current address: Harvard-Smithsonian Center for Astrophysics, 60 Garden Street, Cambridge, MA 02138; bellm@fas.harvard.edu.
[2] Current address: Enrico Fermi Institute, University of Chicago, 5640 South Ellis Avenue, Chicago, IL 60637; johnv@oddjob.uchicago.edu.

TABLE 1
BAND CROSS SECTIONS

Band	Energy[a] (eV)	Cross Section[b] (10^{-20} cm^2)	Reference
Be	73–111	10.5	1
B	115–188	1.7	2
R1	110–284	1.4	3
R2	140–284	0.86	3
R12	120–284	1.0	3

[a] 10% of peak response. Plots of the band response are given in Fig. 1.
[b] Cross section to radiation from $\sim 10^6$ K thermal plasma.
REFERENCES.—(1) Juda et al. 1991; (2) McCammon et al. 1983; (3) Snowden et al. 1997.

for the behavior of the softer bands. S98 checked for consistency with the Be-band observations, but in this paper we investigate whether a more complete analysis with all of the available low-energy data adds support for their model.

In §§ 2 and 3 we compare the behavior in the B and Be bands to what would be expected from the specific halo/local division found by the analysis of S98. In § 4 we investigate whether all the observed band ratios (B/R12, Be/R12, and R1/R2) can be fit by a single-temperature emission model. We find that with current collisional ionization equilibrium models, depleted abundances are necessary to achieve even rough consistency with the observed band ratios. We also show that the fitted model parameters depend strongly on the particular model.

2. ISOLATING LOCAL EMISSION

At Be-band energies, almost complete extinction is produced by even the smallest observed column densities of neutral hydrogen ($\sim 10^{19}$ cm^{-2} for unit optical depth; Table 1). Since all Be-band measurements were made toward regions with $N_{\rm H} = (1\text{–}6) \times 10^{20}$ cm^{-2} (Schlegel et al. 1998), virtually all Be-band counts must originate from the LHB. The smaller cross section for R12 photons (Table 1) means that a larger fraction of the counts in that band may be nonlocal. Juda et al. (1991) found only negligible column densities ($\sim 10^{18}$ cm^{-2}) of $N_{\rm H}$ intermixed in the LHB in their best fit to the Be-band data.

Accordingly, the ratio of the Be-band counts to R12 counts produced locally should be constant for uniform conditions in the LHB. As noted by S98, their modeled local R12 rates display this expected correspondence with the Be-band observations, but similar conclusions were reached using the total $\frac{1}{4}$ keV flux during early analysis of the Be-band data, which had supported the LHB-only model (Bloch et al. 1986). To make a direct comparison, we obtained total (Snowden et al. 1997) and local (S98) R12-band rates in the directions of the 25 Be-band measurements by averaging over the 15° FWHM fields of the rocket observations. We have excluded directions that overlap atypical features in the X-ray maps, such as the Eridanus enhancement, the Monogem ring, the Cygnus superbubble, the Vela supernova remnant (SNR), and the North Polar Spur (see Snowden et al. 1995). We have also excluded a region of enhanced $N_{\rm H}$ where there exists evidence for Be-band absorption ($l = 132\overset{\circ}{.}6$, $b = -76\overset{\circ}{.}8$; Edwards 1990; Burrows et al. 1984).

Comparing the plots in Figures 2*a* (Be vs. local R12) and 2*b* (Be vs. total R12), we see that the Be rates have a noticeably better linear correspondence with just the local part of the R12 rates than they do with the total R12 rates. That is, a linear fit to the Be versus R12 rates yields a smaller χ^2 for the local R12 rates than for the total R12 rates. The Be-to–total-R12 ratios are consistently low in just those directions where there is a large halo contribution in the S98 two-component model.

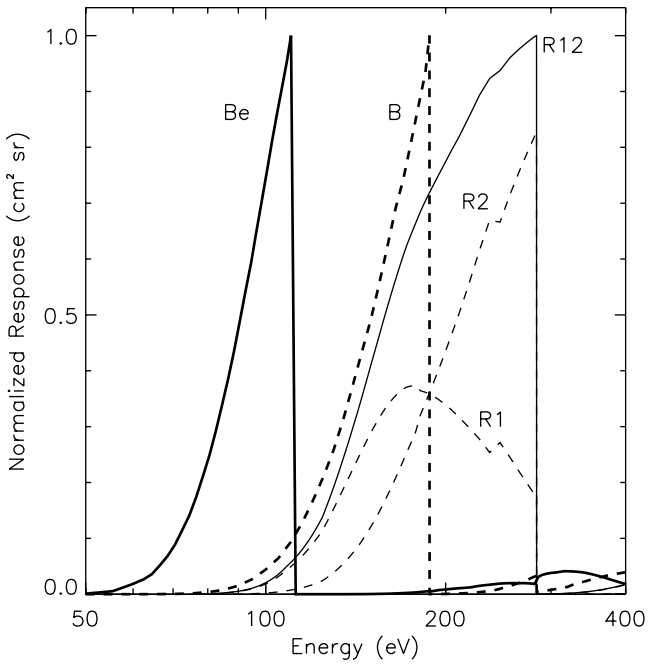

FIG. 1.—Normalized response functions for the pulse-height bands considered in this work. The B and Be bands are from the sounding rocket investigations of McCammon et al. (1983), Bloch et al. (1986), Edwards (1990), and Juda et al. (1991). The R1, R2, and R12 (≡R1 + R2) bands are from the *ROSAT* satellite (Snowden et al. 1994b, 1997); these three bands are normalized to the peak of the R12 band.

3. CORRELATIONS WITH COLUMN DENSITY

3.1. *Energy Dependence of Absorption*

The two-component model also makes definite predictions for changes in the spectral distribution of the distant component with $N_{\rm H\,I}$ due to energy-dependent absorption. We estimated the observed intensity of the halo emission in the R1, R2, R12, and B bands by subtracting the local rates in each band from the total observed rate. The local R1 and R2 rates were taken from the S98 fits. For the B band, the local R12 map was first scaled by the observed low-latitude B/R12 ratio (∼0.11; with B-band units of counts s^{-1} and R12-band units of 10^{-6} counts s^{-1} arcmin^{-2}) to obtain an estimate of the local B-band rate. This local rate was subtracted from the observed total B-band map of the Wisconsin sky survey (McCammon et al. 1983) to determine observed B-band counts ostensibly from the halo. For this study we have binned the all-sky data into $15^\circ \times 15^\circ$ sections and limited the observations to those at high Galactic latitudes ($|b| > 45^\circ$), as the lower latitude points are dominated by LHB emission. We have also excluded the atypical regions discussed in § 2 and regions where the B band was contaminated by electrons or X-rays produced in the solar wind or terrestrial atmosphere (McCammon et al. 1983).

For S98's assumed uniform halo emission spectrum, the R1/R2 and B/R12 band ratios for the observed halo component should vary in a predictable way with absorbing column density. The hydrogen column density in each direction was determined by scaling the 100 μm fluxes of Schlegel et al. (1998) by a factor of 1.475×10^{20} cm^{-2} MJy^{-1} sr (determined by Kuntz & Snowden 2000) and averaging over the sky bin.

Figure 3 shows the band ratios for these fields versus H I column density. We have also plotted the ratios expected from the

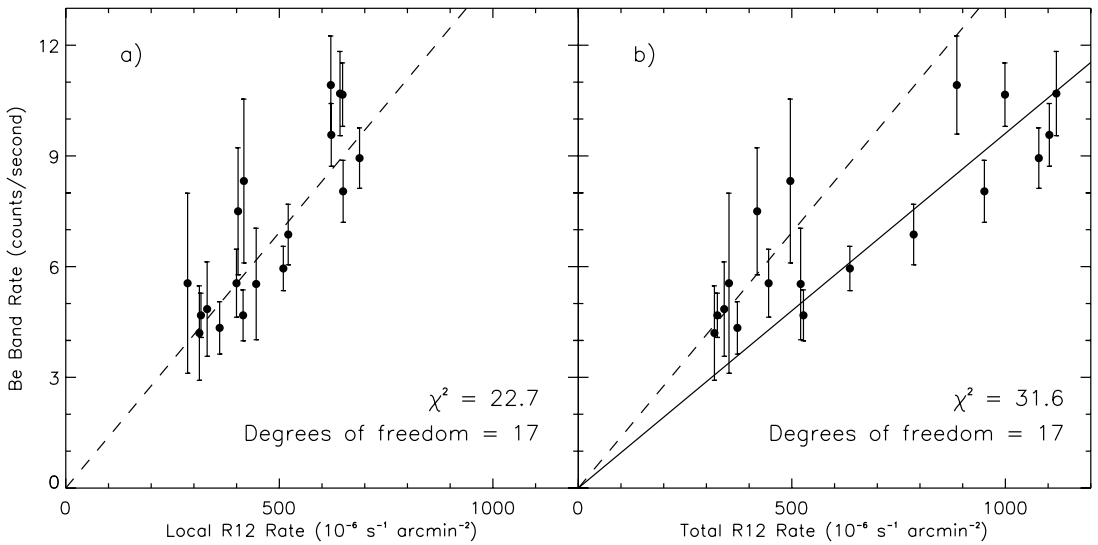

FIG. 2.—(*a*) Wisconsin Be-band counts vs. local R12 rate predicted by the model of Snowden et al. (1998). The best-fit slope of 0.0139 is shown as a dashed line. (*b*) Wisconsin Be-band counts vs. total R12 rate. The best-fit slope of 0.0096 is shown as a solid line. The dotted line is the best-fit slope from (*a*). Regions of the sky with atypical X-ray flux features have been excluded (see text).

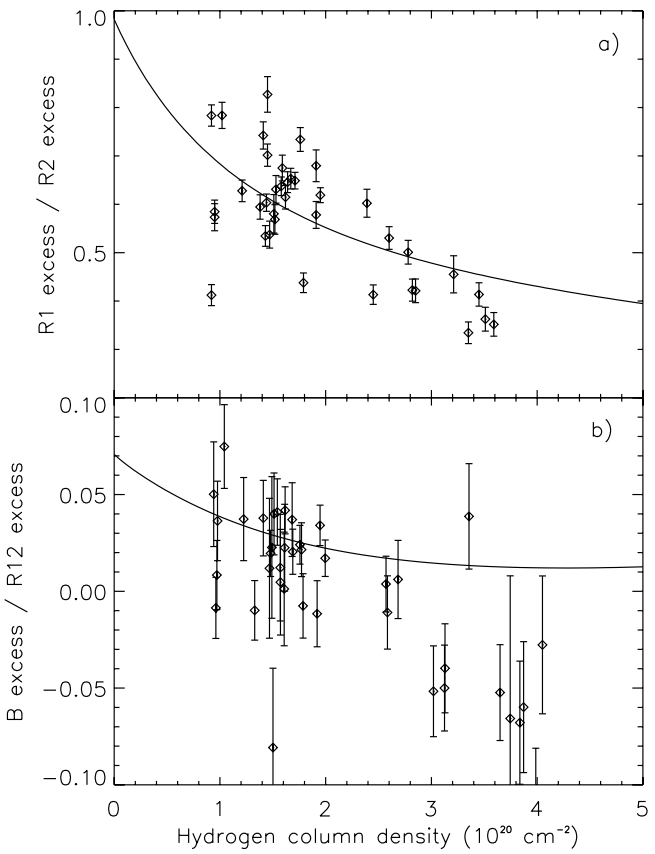

FIG. 3.—Band ratios of absorbed halo emission inferred from the Snowden et al. (1998) model vs. neutral hydrogen column density. Data at low Galactic latitudes ($|b| < 45^\circ$) have been excluded. The ratio predicted by the Snowden et al. model is shown by the solid curves. Absorbed count rates were obtained by subtracting the modeled local count rates from the total observed rates for $15^\circ \times 15^\circ$ bins on the sky. (*a*) Ratio of the *ROSAT* R1 band to the R2 band. (*b*) Ratio of the B band to the R12 band. The error bars in (*b*) take into account only the uncertainties of the B-band measurements; the R12 uncertainties are small compared to those in the B band. The barely perceptible rise in the model curve at high $N_{\rm H}$ in (*b*) is due to a "leak" in the B-band response at ~400 eV, which is larger than that in the R12 band (see Fig. 1).

plasma emission model of Raymond & Smith (1977) at a plasma temperature of $\log T = 6.02$ (S98's modeled halo temperature). (This model was implemented in XSPEC,[3] version 11.2 [e.g., Arnaud 1996]; see § 4). These plots are very "noisy" because subtraction of the large local component leaves the residual dominated by statistical errors and by small deviations from the uniform assumptions of the model. Nonetheless, the ratios do display the expected trends with column density and are not consistent with the LHB-only model, in which the thickness of the disk H I should have no effect on the spectrum.

As a corollary to this, the unabsorbed intensity of halo emission should be independent of foreground column density. This is a rather strong test, since the halo intensities are computed by dividing the observed halo component by the calculated gas transmission, a large correction that is itself directly correlated with column density. Kuntz & Snowden (2000) performed this test, and their Figure 4 appears remarkably uncorrelated.

3.2. *Relative Local/Halo Flux Contributions*

Because of the large interstellar absorption, the halo component contributes only about 11% to the average observed intensity in the R12 band. However, in a few directions where the column density is low and the halo happens to be bright, it dominates the total emission, and it must contribute strongly to the observed anticorrelation with H I. In Figure 4 we plot the rates in the *ROSAT* R12 band versus $N_{\rm H}$ (again, the data have been binned in $15^\circ \times 15^\circ$ sections on the sky). The data points labeled "local" are the LHB emission as modeled by S98, while the "observed halo" rates are the actual total rates minus the local rates. Both are strongly anticorrelated with H I column density. For the halo component, this should result from absorption, and for the LHB component it is presumably because of displacement. The two effects can be seen to contribute about equally to the observed anticorrelation.

3.3. *Solar Wind Charge Exchange*

The anticorrelation of local R12 with $N_{\rm H}$ also provides a constraint on the portion of the local flux that may be attributed to

[3] Available at http://heasarc.gsfc.nasa.gov/docs/xanadu/xspec/.

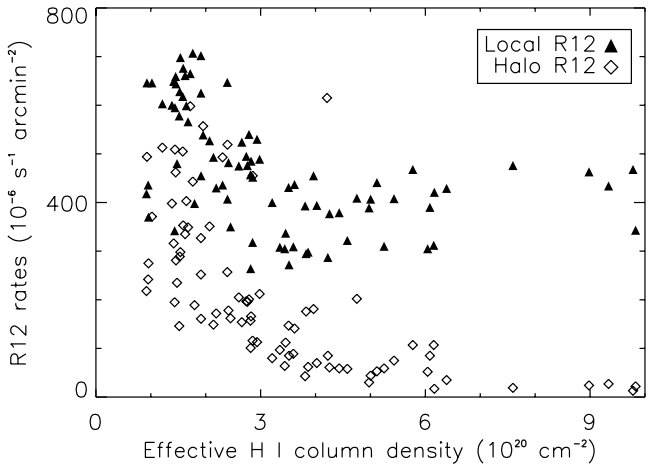

FIG. 4.—Local Hot Bubble (Snowden et al. 1998) and observed halo (≡total − LHB) rates in the *ROSAT* R12 band vs. column density. Both components contribute about equally to the observed X-ray–$N_{\rm H\,I}$ anticorrelation. This also implies that at least some of the LHB emission is not local to the solar system. Error bars are approximately the same size as the data points. All Galactic latitudes are included in this plot, but we have excluded the same contaminated and atypical regions of the sky as in Figs. 2 and 3.

solar wind charge-exchange emission (CXE). Since the CXE should not be correlated with the Galactic disk H I column density, the $N_{\rm H\,I}$–dependent portion in Figure 4 implies a nonzero contribution to this flux from a LHB. The magnitude of the $N_{\rm H\,I}$–independent portion is consistent with the results of Lallement (2004), who puts an upper limit of $\sim 300 \times 10^{-6}$ counts s^{-1} arcmin^{-2} on CXE. Since the all-sky average of the S98 local component is 455×10^{-6} counts^{-1} arcmin^{-2} (Fig. 4), at least 34% of it must originate in an extensive LHB.

4. CONSTRAINTS ON SPECTRAL MODELS

In a more sophisticated analysis of the S98 model, Kuntz & Snowden (2000) derived an emission temperature of $\sim 10^{6.1} \pm 10^{0.1}$ K for the LHB. The halo component was consistent with the same temperature but had larger variations. For the halo emission, the small contribution to the observed brightness in the B and Be bands means that there is little information to be added by using these older data. However, in the LHB the low-energy data add a considerable amount of spectral information. Fits to each of these bands to thermal emission models have been done before (e.g., Sanders et al. 2001), but it is worthwhile to revisit the issue using newer spectral models.

At low Galactic latitudes, large absorbing columns ensure that all counts observed at $\frac{1}{4}$ keV and below are generated in local source material. From low-latitude observations, we estimate B/R12 = 0.115. From the fit of Be-band counts to S98's local component, we find Be/R12 = 0.0139 (see Fig. 2*a*). (This Be/R12 ratio is consistent with the value obtained by calculating the ratio of Be to total observed R12 for the limited number of available low-latitude fields.) Figure 5 compares these ratios with the single-temperature collisional ionization equilibrium (CIE) model of Raymond & Smith, implemented in XSPEC, version 11.2. (This version is consistent with that used by S98.) Assuming solar abundances, this model gives quite different temperatures for the three band ratios. We find $\log T = 5.8$ for B/R12 and 6.2 for Be/R12, whereas S98 found $\log T = 6.1$ from the R1/R2 ratio (see Fig. 5; Table 2).

Figure 5 also shows the predicted band ratios for models in which the heavy elements have been depleted with respect to their solar abundances, again using the Raymond & Smith CIE

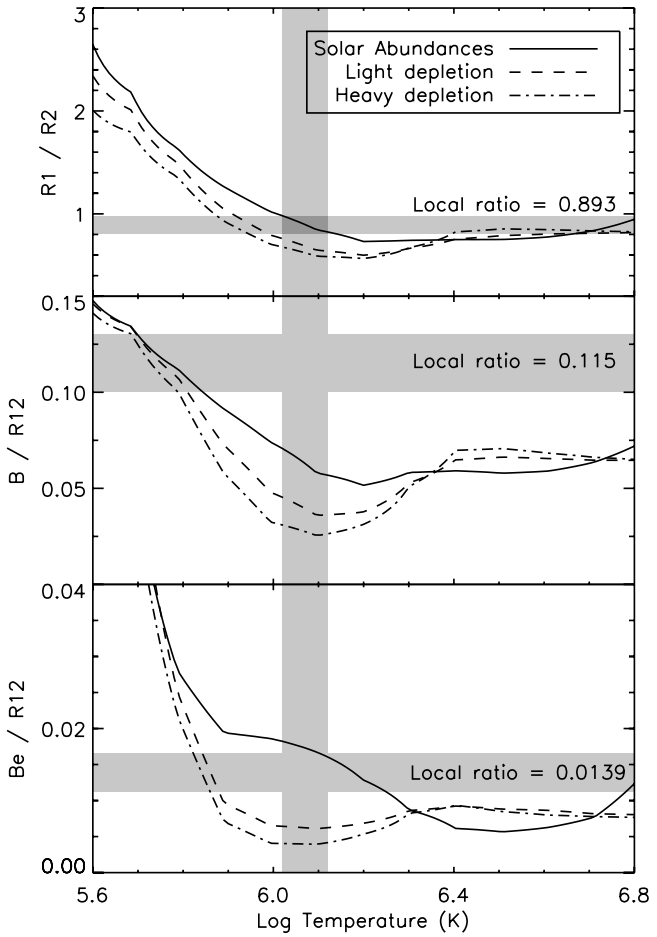

FIG. 5.—Band ratios as a function of plasma temperature. We have used the collisional ionization equilibrium model of Raymond & Smith (1977; implemented in XSPEC, ver. 11.2) to determine the ratio of X-ray emission in the bands in Fig. 1. We compare three sets of elemental abundances tabulated by Savage & Sembach (1996): solar abundances, those observed toward warm (light depletion) clouds, and those observed toward cool (heavy depletion) clouds. The ratios observed at low Galactic latitudes are shown as horizontal gray bands; the widths represent only estimates of the measured ratio's distribution but are not formal errors. The local R1/R2 ratio is from S98, the B/R12 and Be/R12 (see Fig. 2) ratios are from this work. The vertical gray band centered at $\log T = 6.07$ indicates the best-fit temperature to the R1/R2 ratio obtained by S98 using the Raymond & Smith model with solar abundances.

model. The depleted models use abundances observed in a warm cloud (light depletion) and a cold cloud (heavy depletion) toward ζ Oph (Savage & Sembach 1996). None of these models yield entirely consistent temperatures for all three band ratios (see Table 2), but the depleted abundances fare much better than solar, with the heavy depletion model giving the smallest scatter and a temperature near $\log T = 5.84$. One might think that all dust grains should be evaporated in a 10^6 K plasma, and that it is therefore reasonable to consider only solar abundances. However, calculations of grain destruction in shocks and by hot gas sputtering show that over the broad range of feasible histories for the LHB, the surviving fraction of silicate dust mass ranges from >90% for solid grains after 10^6 yr down to 30% for fluffy grains after 10^7 yr (Smith et al. 1996, and references therein). Initial depletions onto the silicate grains are well over 95% for Si and Mg, which are the important emitters in the R12 and B bands, and about 99% for Fe, which dominates the Be band, so final depletions are effectively just the surviving fraction of dust mass. An additional complication of dust is that while sputtering is taking place, cooling is enhanced and the

TABLE 2
MODEL TEMPERATURES ($\log T$) FOR MEASURED BAND RATIOS

Abundances[a]	R1/R2	B/R12	Be/R12	Mean[b]
Solar	6.07 ± 0.05	5.78 ± 0.08	6.19 ± 0.02	6.15 ± 0.21
Light depletion	5.95 ± 0.03	5.75 ± 0.05	5.87 ± 0.02	5.88 ± 0.10
Heavy depletion	5.90 ± 0.04	5.74 ± 0.04	5.84 ± 0.01	5.84 ± 0.08

NOTE.—Temperatures and uncertainties derived from overlap of Raymond & Smith model with measured local band ratios; see Fig. 5.
[a] Abundances from Savage & Sembach (1996); see text.
[b] The mean represents the weighted average of the preceding three columns, while the uncertainty is the standard deviation of the same.

spectrum altered by lines of the underionized atoms recently added to the gas phase.

Bragg crystal spectrometer measurements at low Galactic latitudes with considerably better energy resolution found that the LHB emission was not acceptably fit either by a single-temperature CIE or by any reasonable non-CIE model, but that moderate to heavy depletions of Si and Mg at least offered considerable improvement (Sanders et al. 2001). Observations with microcalorimeters at high latitudes produced qualitatively similar results (McCammon et al. 2002). A recent high spectral resolution observation of the EUV diffuse background by the *Cosmic Hot Interstellar Plasma Spectrometer* (*CHIPS*) satellite has placed upper limits on the Fe lines near 72 eV that would require Fe depletion of at least 10 times to be consistent with a single hot plasma as the source of the soft X-ray flux in the R12 and B bands (Hurwitz et al. 2005). Their best-fit temperature is $\log T = 5.9$, in reasonable agreement with our depleted abundance fits to the soft X-ray bands.

However, single-temperature CIE emission is an idealization of any possible astrophysics, and there are other likely contributors to the observed X-rays, such as charge exchange of solar wind ions in interplanetary space (Lallement 2004), so the actual situation is probably not this simple. While all of these data are consistent with an origin in a single hot plasma, they by no means rule out a substantial contribution from interplanetary charge exchange.

In Figure 6 we compare band ratios calculated with Raymond & Smith and two other widely used equilibrium emission models: MEKAL (Mewe et al. 1985, 1986) and APEC[4] (Smith et al. 2001), both also as implemented in XSPEC version 11.2. All used the cold cloud (heavily depleted) abundances. It can be seen that temperatures derived for a given band ratio have a very significant dependence on the model.

5. SUMMARY

Sounding rocket data in the low-energy B and Be bands add support for the Snowden et al. (1998) model in which the source of the $\frac{1}{4}$ keV diffuse background is composed of both a local unabsorbed component and a very patchy "halo" component absorbed by neutral gas in the Galaxy. Although the halo emission measure is quite large in some directions, its contribution to the observed flux is modest because of the heavy absorption in most directions. Averaged over the sky, the halo component is responsible for only 10.7% of the *ROSAT* R12 band, 4.7% of the B band, and 0.4% of the Be band. However, it supplies more than half the observed intensity in selected directions and is responsible for about half of the anticorrelation with $N_{\rm H\,I}$. Displacement effects in the LHB presumably account for the remainder. The X-ray–$N_{\rm H\,I}$ anticorrelation in the local R12 flux implies that at least 34% of this flux must come from hot gas in the LHB rather than charge exchange reactions in the solar wind.

We also find that Raymond & Smith collisional ionization equilibrium models require depleted abundances to come close to providing a single-temperature solution for the observed Be/R12 and B/R12 band ratios in the Local Hot Bubble. A temperature of $\log T \sim 5.84$ with heavy depletions is most consistent with both these and S98's modeled R2/R1 ratio in the LHB, for which they had found $\log T = 6.07$ using solar abundances. However, other available CIE emission models give quite different results, which does little to lend confidence to what may be a fortuitous fit. The very few available observations of the $\sim\frac{1}{4}$ keV diffuse background with better spectral resolution also favor depleted abundances but suggest that the spectral picture is more complex than single-temperature plasma emission. More realistic astrophysical situations and contributions from other sources, such as solar wind charge exchange, are likely to be parts of the picture. Disentangling and characterizing these will almost surely require measurements of individual line intensities and physical analysis of their ratios rather than modeling of broadband rates.

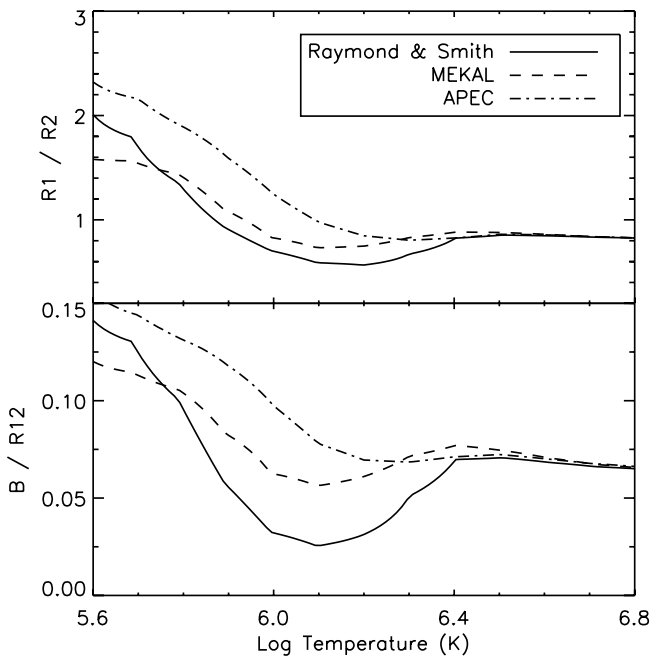

FIG. 6.—Band ratios as a function of temperature for different models of equilibrium plasmas, all using heavily depleted elemental abundances (as in Fig. 5).

[4] See http://cxc.harvard.edu/atomdb/sources_apec.html.

We would like to thank Steve Snowden for providing the maps of his model of the $\frac{1}{4}$ keV flux and Kip Kuntz for providing the Raymond & Smith spectrum used by Snowden et al. 1998. We would also like to thank Dan McCammon and Wilt Sanders for useful discussions, direction, and assistance with data analysis and interpretation. This work was supported by a NSF-REU site grant (AST 01-39563) to the University of Wisconsin–Madison and E. C. B. and by NASA grant NAG5-5404.

REFERENCES

Arnaud, K. A. 1996, in ASP Conf. Ser. 101, Astronomical Data Analysis Software and Systems V, ed. G. H. Jacoby & J. Barnes (San Francisco: ASP), 17
Bloch, J. J., Jahoda, K., Juda, M., McCammon, D., Sanders, W. T., & Snowden, S. L. 1986, ApJ, 308, L59
Burrows, D. N., McCammon, D., Sanders, W. T., & Kraushaar, W. L. 1984, ApJ, 287, 208
Burrows, D. N., & Mendenhall, J. A. 1991, Nature, 351, 629
Edwards, B. C. 1990, Ph.D. thesis, Univ. Wisconsin, Madison
Hurwitz, M., Sasseen, T. P., & Sirk, M. M. 2005, ApJ, in press (astro-ph/0411121)
Juda, M., Bloch, J. J., Edwards, B. C., McCammon, D., Sanders, W. T., Snowden, S. L., & Zhang, J. 1991, ApJ, 367, 182
Kuntz, K. D., & Snowden, S. L. 2000, ApJ, 543, 195
Lallement, R. 2004, A&A, 418, 143
McCammon, D., Burrows, D. N., Sanders, W. T., & Kraushaar, W. L. 1983, ApJ, 269, 107
McCammon, D., & Sanders, W. T. 1990, ARA&A, 28, 657
McCammon, D., et al. 2002, ApJ, 576, 188
Mewe, R., Gronenschild, E. H. B. M., & van den Oord, G. H. J. 1985, A&AS, 62, 197
Mewe, R., Lemen, J. R., & van den Oord, G. H. J. 1986, A&AS, 65, 511
Raymond, J. C., & Smith, B. W. 1977, ApJS, 35, 419
Sanders, W. T., Edgar, R. J., Kraushaar, W. L., McCammon, D., & Morgenthaler, J. P. 2001, ApJ, 554, 694
Sanders, W. T., Kraushaar, W. L., Nousek, J. A., & Fried, P. M. 1977, ApJ, 217, L87
Savage, B. D., & Sembach, K. R. 1996, ARA&A, 34, 279
Schlegel, D. J., Finkbeiner, D. P., & Davis, M. 1998, ApJ, 500, 525
Smith, R. K., Brickhouse, N. S., Liedahl, D. A., & Raymond, J. C. 2001, ApJ, 556, L91
Smith, R. K., Krzewina, L. G., Cox, D. P., Edgar, R. J., & Miller, W. W. I. 1996, ApJ, 473, 864
Snowden, S. L., Cox, D. P., McCammon, D., & Sanders, W. T. 1990, ApJ, 354, 211
Snowden, S. L., Egger, R., Finkbeiner, D. P., Freyberg, M. J., & Plucinsky, P. P. 1998, ApJ, 493, 715 (S98)
Snowden, S. L., Hasinger, G., Jahoda, K., Lockman, F. J., McCammon, D., & Sanders, W. T. 1994a, ApJ, 430, 601
Snowden, S. L., McCammon, D., Burrows, D. N., & Mendenhall, J. A. 1994b, ApJ, 424, 714
Snowden, S. L., Mebold, U., Hirth, W., Herbstmeier, U., & Schmitt, J. H. M. 1991, Science, 252, 1529
Snowden, S. L., et al. 1995, ApJ, 454, 643
———. 1997, ApJ, 485, 125